628

Growth of iron on iron whiskers

Joseph A. Stroscio and D. T. Pierce
Electron Physics Group, National Institute of Standards and Technology, Gaithersburg, Maryland 20899

(Received 9 August 1993; accepted 1 December 1993)

Real space views of the homoepitaxial growth of Fe on Fe(001) whiskers is reported, observed by scanning tunneling microscopy (STM), during the initial stages of growth. Scaling of the Fe island sizes and separation distributions are observed as a function of the diffusion rate to the deposition rate. A measure of the surface diffusion of the Fe atoms is obtained over the temperature range of 20–250 °C from the temperature dependence of the island density. The effect of the diffusion kinetics is also observed in the surface morphology as a decrease in surface roughness with increasing temperature in thin Fe films. A comparison of real and reciprocal space techniques is obtained from a comparison of STM images and reflection-high-energy-electron-diffraction measurements during growth.

I. INTRODUCTION

In this article, we summarize some observations of MBE growth of Fe on single crystal Fe(001) whiskers studied by scanning tunneling microscopy (STM) and reflection high-energy electron diffraction (RHEED) measurements.[1,2] Measurements are reported, ranging from the initial nucleation of islands to multilayer film growth. In the initial stages of growth, island formation is observed and detailed measurements of the density, size, and pair separation distributions are obtained from STM measurements. Scaling of the size and separation distributions as a function of diffusion to deposition rate, at fixed coverage, are observed in the growth temperature range of 20–200 °C, and support recent theories of growth emphasizing scaling behavior in these quantities.[3,4] RHEED measurements during growth are compared with the surface morphology, and give insight into the interpretation of RHEED intensity oscillation behavior.

The experiments were performed in an ultrahigh vacuum system with STM and RHEED measurement capability and molecular beam epitaxy (MBE) facilities for metal film growth.[5] RHEED measurements were made with a 10 keV electron beam and acquired by digitally recording the diffraction patterns in real time during growth. Fe was evaporated using an e-beam heated source with the substrate held at some temperature, and then cooled after growth for analysis by STM measurements at room temperature. The STM measurements were made with single crystal (111) oriented W tips. The tips were cleaned and prepared using field ion and electron emission techniques yielding reproducibly sharp tips with radii of ~10 nm. The substrates for growth were Fe single crystal whiskers,[6] cleaned by sputtering at 750 °C. A *typical* image of an Fe whisker surface is shown in Fig. 1(a). Monatomic steps separated by ~1 μm are observed across the whisker. The dominant defects on the surface are screw dislocations [see the arrows in Fig. 1(a)], which are seen to originate the steps. A close view of the surface, shown in Fig. 1(b), shows the 1×1 Fe lattice with 0.287 nm spacing. The corrugation amplitude of the 1×1 surface is typically a few pm at a tunneling resistance of ~10^9 Ω.

II. SCALING IN THE INITIAL STAGES OF ISLAND GROWTH

A microscopic understanding of the processes of diffusion, nucleation, and growth is central for developing theories of growth. While the observation of the diffusion of individual atoms is beyond the standard STM measurement, much insight can be gained from analyzing "snapshots" during the growth process.[4] The process of film growth involves the deposition of atoms on the surface, which initially increases the density of mobile adatoms beyond their equilibrium value. The adatoms diffuse and collide with other adatoms to form a stable nucleus for island growth. Once islands form, there is a competition between the processes of nucleation of the mobile adatoms into additional islands and the growth of existing islands by incorporating the mobile adatoms. The time scale for these events depend on the surface diffusion rate and the deposition rate. In the temperature range considered here, the formation of islands can be considered essentially irreversible due to the higher activation energy for an atom to desorb from an island compared to diffusing along the surface.[3] For this irreversible island formation, a number of island parameters have been predicted to show scaling behavior as a function of diffusion to deposition rate,[3] which have been directly observed in this study. A knowledge of how island density scales with the surface diffusion rate, for example, allows a determination of the activation energy for diffusion from the temperature dependence of the island density.

We begin by depositing Fe on the Fe(001) whisker surfaces (see Fig. 1) at a rate r, for a fixed time, to yield the same total flux (or coverage) as a function of substrate temperature, thereby varying the surface diffusion rate D. The number of jumps an atom makes on the surface per second, which is the hopping rate h, is related to the diffusion constant by $D=ha^2$, where a is the lattice constant. A series of STM images, at different growth temperatures, for the same coverage of 0.07±0.016 ML (monolayer) is shown in Fig. 2. The competition between nucleation and growth is seen to depend strongly on temperature. Growth is favored at higher temperatures, where the adatoms can diffuse longer distances to find an existing island before nucleating another island. Three aspects are immediately apparent from the images of

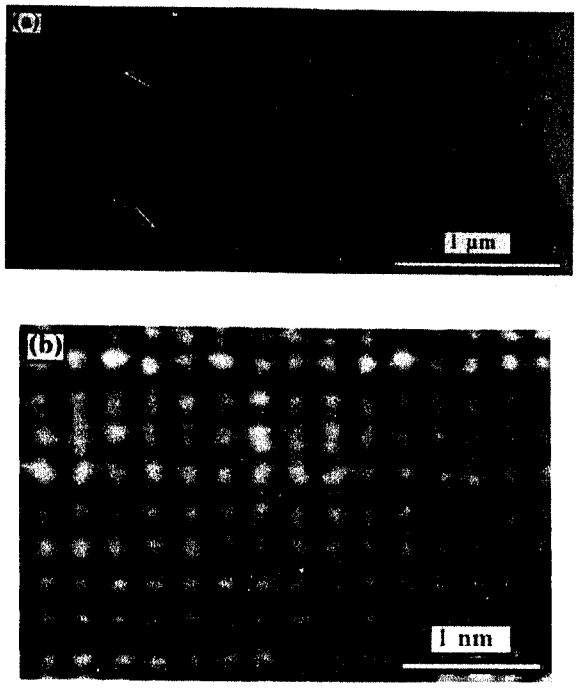

FIG. 1. STM images of the clean Fe(001) whisker surface. (a) Large view, 3.5×1.6 μm, showing the typical surface step density. Arrows indicate positions of screw dislocations; (b) close-up view, 4×3 nm, showing 1×1 atomic lattice.

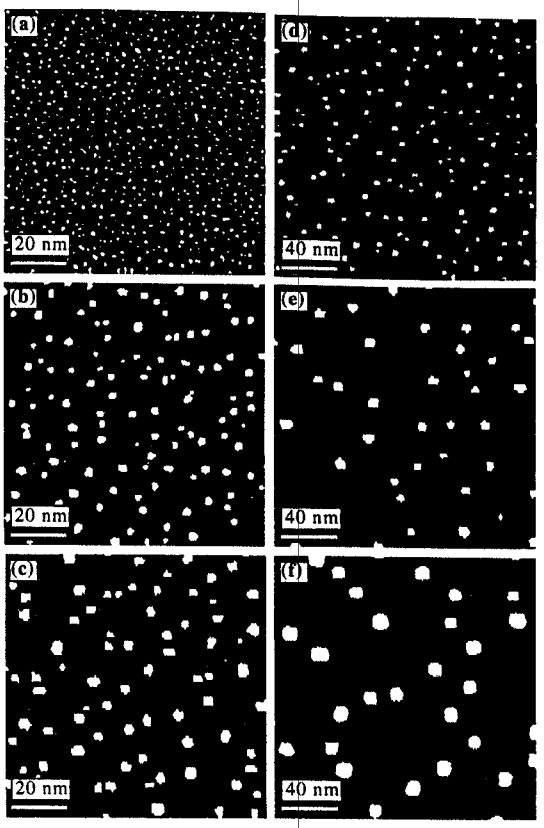

FIG. 2. STM images, 100×100 nm, of single layer Fe islands (white) on the Fe(001) surface (black). Sample temperatures during growth are (a) 20 °C; (b) 108 °C; (c) 163 °C; (d) 256 °C; (e) 301 °C; and (f) 356 °C. Fe was deposited for a fixed time for all measurements with a flux of $1.4\pm0.3\times10^{13}$ atoms $cm^{-2}\,s^{-1}$, yielding a coverage of 0.07 ± 0.016 ML (1 ML $=1.214\times10^{15}$ atoms cm^{-2}).

the islands in Fig. 2. First, the island density decreases with increasing temperature. Second, there is a characteristic distance around each island, which is void of other islands. Third, the self-similarity of the size distributions is suggested by comparing the images of Figs. 2(a)–2(c), with those of Figs. 2(d)–2(f), where the scale length is a factor 2 different.

The island density in Fig. 3 shows an Arrhenius dependence on temperature due to the activated process of surface diffusion for temperatures <250 °C. Above this temperature, a sharp decrease in island density is observed. The so-called tracer diffusion coefficient[7] of single adatoms can be extracted from the data in Fig. 3, using a knowledge of the scaling of island density to diffusion constant. A number of studies have shown that he island density scales at $N\sim(h/r)^{-\chi}$ for $h/r\gg1$, and $\chi=1/3$ in two dimensions.[3,4] Deviation from $\chi=1/3$ for general h/r can be obtained from a rate equation analysis, which applied to the data in Fig. 3 for $T\leqslant250$ °C, yields the temperature dependence of the diffusion constant, shown in Fig. 4.[1,2] Assuming an Arrhenius form for the diffusion constant, $D=D_0e^{-E/kT}$, one obtains the activation energy for diffusion.

The island sizes vary greatly as a function of temperature due to the tendency toward growth with increasing temperature (see Fig. 2). Bartelt *et al.* have developed a scaling theory for the full island size distribution and propose the scaling relation for large h/r,[3]

$$N_s\sim\theta s_{\rm av}^{-2}f(s/s_{\rm av}), \tag{1}$$

where N_s is the density of islands per lattice site of size s atoms. The average island size is defined by

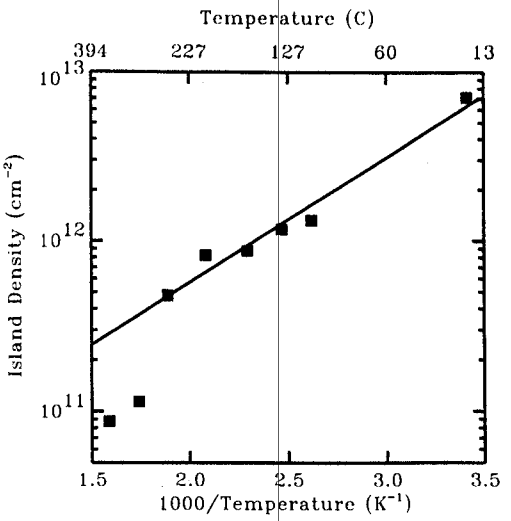

FIG. 3. The temperature dependence of the density of Fe islands obtained from STM measurements as in Figs. 2(a)–2(f). The solid line is at least squares fit for $T\leqslant250$ °C.

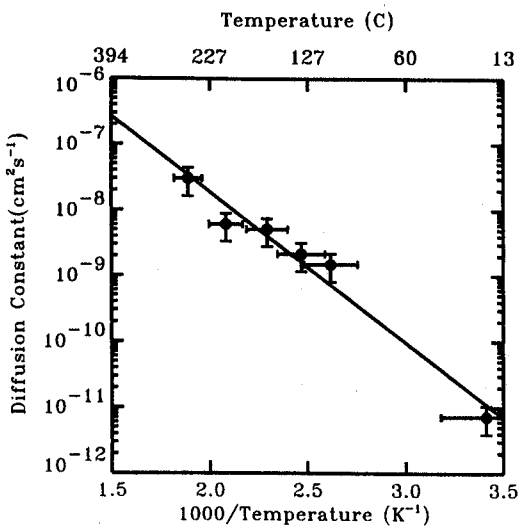

FIG. 4. The temperature dependence of the diffusion constant obtained from a rate equation analysis of the island density in Fig. 3. The solid line is a least squares fit to an Arrhenius form $D=D_0e^{-E/kT}$, yielding an activation energy for diffusion, $E=0.45\pm0.08$ eV, and a prefactor $D_0=7.2\times10^{-4}$ cm^2 s^{-1}.

$$s_{\rm av}=\sum_{s\geq1} sN_s \Big/ \sum_{s\geq1} N_s=\frac{\theta}{(N+N_1)}\sim\frac{\theta}{N}, \qquad (2)$$

since the relative number of monomers, N_1, is small compared to the total number of islands, $N(s\geq2)$. In our analysis, we are assuming that a stable island nucleus consists of two or more atoms, which is justified by the following scaling analysis of the island size distributions.

Figure 5 shows the scaled Fe island size distributions obtained from the STM images over the temperature range of 20–356 °C, which corresponds to h/r ranging from 10^6–10^{10}. As seen in Fig. 5(a), the scaling of the distributions holds well for temperatures <250 °C; all the distributions collapse onto a single curve, which verifies the theory of Bartelt *et al.*[3] The resulting scaling function in Fig. 5(a) agrees well with the simulations results of Bartelt *et al.*[3] for a critical nucleus size of 1, which implies that a cluster of two or more atoms are stable in this temperature range. At higher temperatures, the scaled distributions in Fig. 5(b) are significantly narrower in width, and have a maximum greater than one. While coarsening due to Ostwald ripening would also tend to narrow the size distribution, we would not expect subsequent distributions at other temperatures to have the same scaled size distribution. Therefore, we attribute this high-temperature distribution to a second scaling function, which may come about by a change in critical size for nucleation.[2] The total island density also showed deviation from simple behavior in this temperature range, as shown in Fig. 3.

In the images of the islands in Fig. 2, one notices a characteristic region around each island, which is void of other islands. This follows from the nucleation probability depending on an adatom finding a nearby adatom, coupled with the fact that the monomer density is zero at the edge of the island and increases as one goes away from the island be-

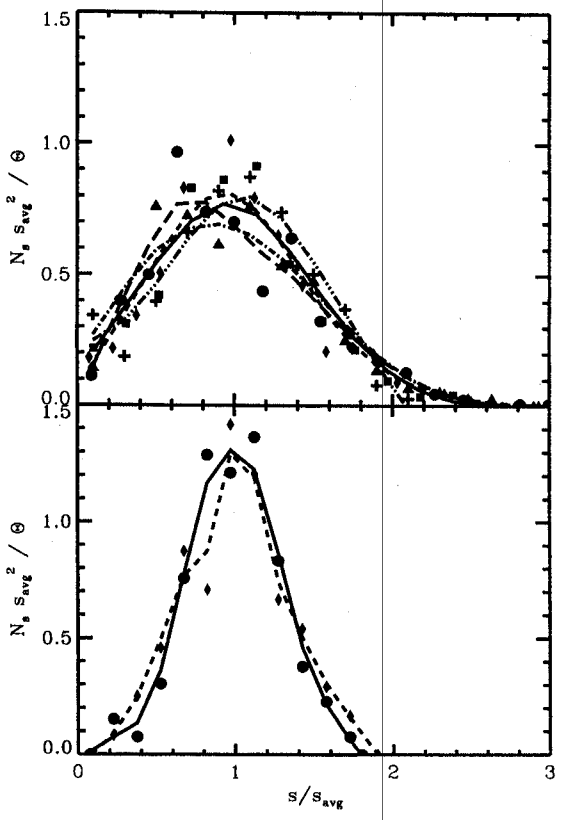

FIG. 5. Scaled island size distributions as a function of growth temperature from the STM measurements as in Fig. 1. N_s is the island density per lattice site of islands with s atoms, and $s_{\rm av}$ is the average island size taken as θ/N, where θ is the total coverage and N and the total island density. The lines are smooth splines to the data points, which are obtained from a histogram of the island distributions. (a) Lower-temperature data; the temperatures and ratio of hopping rate/deposition rate (h/r) are (○,—) 20 °C, 1.2×10^6; (□,––)108 °C, 7.3×10^7; (◇,---) 132 °C, 1.7×10^8; (△,–·–) 163 °C, 4.2×10^8; and (+,–···) 207 °C, 1.3×10^9. (b) Higher-temperature data; (◇,––) 301 °C, 7.7×10^9; (○,—) 356 °C, 1.7×10^{10}.

cause the island acts as a sink for the monomers. This results in a lower nucleation probability in the vicinity of an island. This behavior is observed in the distance dependence of the island separation probability, $N(r)$, defined as the conditional probability of finding an island (of any size) separated by r from a specified island. $N(r)\to N$, as $r\to\infty$. The scaling of the probability distributions has been proposed in the limit of large h/r to be[3]

$$N(\mathbf{r})\sim Ng_N\left(\frac{r-r_0}{l_{\rm av}}\right). \qquad (3)$$

where $l_{\rm av}$ is the characteristic separation between islands, $l_{\rm av}\sim\sqrt{1/N}$, and r_0 is the minimum separation where $N(r)$ vanishes. Here g_N has the property, $g_N\to0, r\to0$ and $g_N\to1, r\to\infty$. Figure 6 shows the scaled radial distribution functions for the Fe data. One observes very good scaling of the radial distribution functions, collapsing onto a single curve. The most notable feature of the distribution is the characteristic depletion of islands at small distances due to the decrease in nucleation probability mentioned above. A functional form for g_N can be obtained from a solution of a

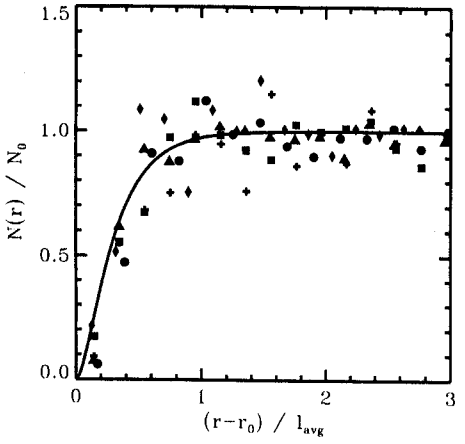

FIG. 6. Scaled radial probability distributions for finding an Fe island separated by a distance r from a given island obtained from the STM images, as in Fig. 2. The growth temperatures and ratio of hopping/deposition rate are (○) 20 °C 1.2×10^6; (□) 108 °C, 7.3×10^7; (◇) 132 °C, 1.7×10^8; (△) 163 °C, 4.2×10^8; and (+) 256 °C, 3.5×10^9. l_{av} is taken as $1/\sqrt{N}$ and r_0/l_{av} as $\sqrt{\theta}$. The solid line is given by $[1-K_0(\lambda(y_0+x))/K_0(\lambda y_0)]^2$, where K_0 is the modified first-order Bessel function, $x=(r-r_0)/l_{av}$, $\lambda=\sqrt{4\pi}$, and $y_0=r_0/l_{av}\sim\sqrt{\theta}=0.26$ (Ref. 3).

diffusion equation,[3] and is shown in Fig. 6. It is remarkable how well a simple theory can predict the functional form of the radial distribution probabilities.

III. GROWING THIN Fe FILMS

The effect of the diffusion kinetics was seen in the temperature dependence of the island densities and sizes. Diffusion kinetics continues to strongly influence film growth as the thickness is increased. One of the main diagnostics of film growth has been RHEED, in which a high-energy (~10–30 keV) electron beam strikes a surface at grazing incidence, and the resulting diffraction pattern is monitored during growth.[8] It was found that the diffraction features oscillate in time during growth, and the oscillations were taken as indicating the addition of successive monolayers to the film.[9] Through detailed modeling of the RHEED oscillations, information about the surface morphology has been deduced.[8] However, the exact origin of RHEED oscillations, has not been fully explained,[1,8,10–12] leading to uncertainty as to what extent the surface morphology can be reliably deduced from RHEED intensity behavior. Our study of Fe on Fe was one of the first studies to correlate different RHEED intensity behavior associated with measured surface morphology on the same samples.[1]

Figure 7 shows STM and RHEED measurements of 5 ML of Fe as a function of temperature. At 20 °C, the higher propensity for nucleation results in a rough film with five exposed layers, as shown in Fig. 7(a). The islands have a mean spacing of approximately 5 nm. This structure gives rise to a splitting of the diffraction beams in the RHEED pattern. The observed splitting of the RHEED diffraction features in Fig. 7(a) is in agreement with simulations calculated from the surface correlation function obtained from the real space STM image in Fig. 7(a).[1,2] Detailed measurements of the surface morphology at this temperature show a surface roughness that increases monotonically with film thickness due to kinetically limited growth,[2] and suggests the decay in the (0,0) RHEED intensity is correlated with surface roughness. A kinematic theory of RHEED predicts the intensity is exponentially dependent on surface roughness.[13,14]

An increased diffusion rate at higher temperature results a larger terrace structure as observed in Fig. 7(b) for the 180 °C growth temperature. The RHEED diffraction features show a broadened component that is observed in Fig. 7(b), due to the terrace structure. The (0,0) RHEED intensity shows stronger oscillations, but still with a significantly damped intensity envelope. Interestingly, the surface roughness is comparable to the growth at 20 °C, and there are still five layers exposed, which supports the theory that roughness is the origin of the RHEED intensity decay for the Fe on Fe system studied here.

Nearly layer-by-layer growth is not observed until the diffusion rate is increased substantially, and is characterized by the RHEED intensity oscillations returning to nearly their initial value, with very little damping, as shown in Fig. 7(c). The surface morphology is seen to consist of three layers with one layer predominant. In addition, the RHEED diffraction features are nearly the same as the starting surface, except for a very small broadened component due to the terrace structure, which is exaggerated in the figure due to the chosen logarithmic intensity scale. Further measurements at this temperature during the RHEED oscillation cycle lend some support to a kinematic description of the intensity oscillations observed in RHEED at the anti-Bragg angles, but cannot explain all RHEED behavior which requires a full multiple scattering theory.[1,8]

IV. CONCLUSIONS

We have shown detailed measurements of the initial growth of Fe on Fe(001) whiskers. At submonolayer coverages below 10%, scaling of the island sizes, and separation distributions were observed as a function of the ratio of diffusion to deposition rate over the range of 10^6–10^9 (20–250 °C), and support recent theories, emphasizing scaling in these quantities with a critical nucleus size of one.[3] At higher temperatures, deviations from the initial scaling behavior is observed. The diffusion constant of single Fe atoms on the Fe(001) surface was obtained from an analysis of the temperature dependence of the Fe island density, and yielded an activation energy for diffusion of $E=0.45\pm0.08$ eV. The effect of diffusion kinetics was also observed in the initial stages of film growth, by STM and RHEED measurements, with a surface roughness decreasing with increasing temperature. RHEED intensity oscillations were correlated with STM surface morphology measurements, which suggested that roughness is an important mechanism for the decay of RHEED intensity oscillations. Nearly layer-by-layer growth, as observed by STM measurements, was shown to be characterized by a RHEED intensity oscillations, which show very little decay.

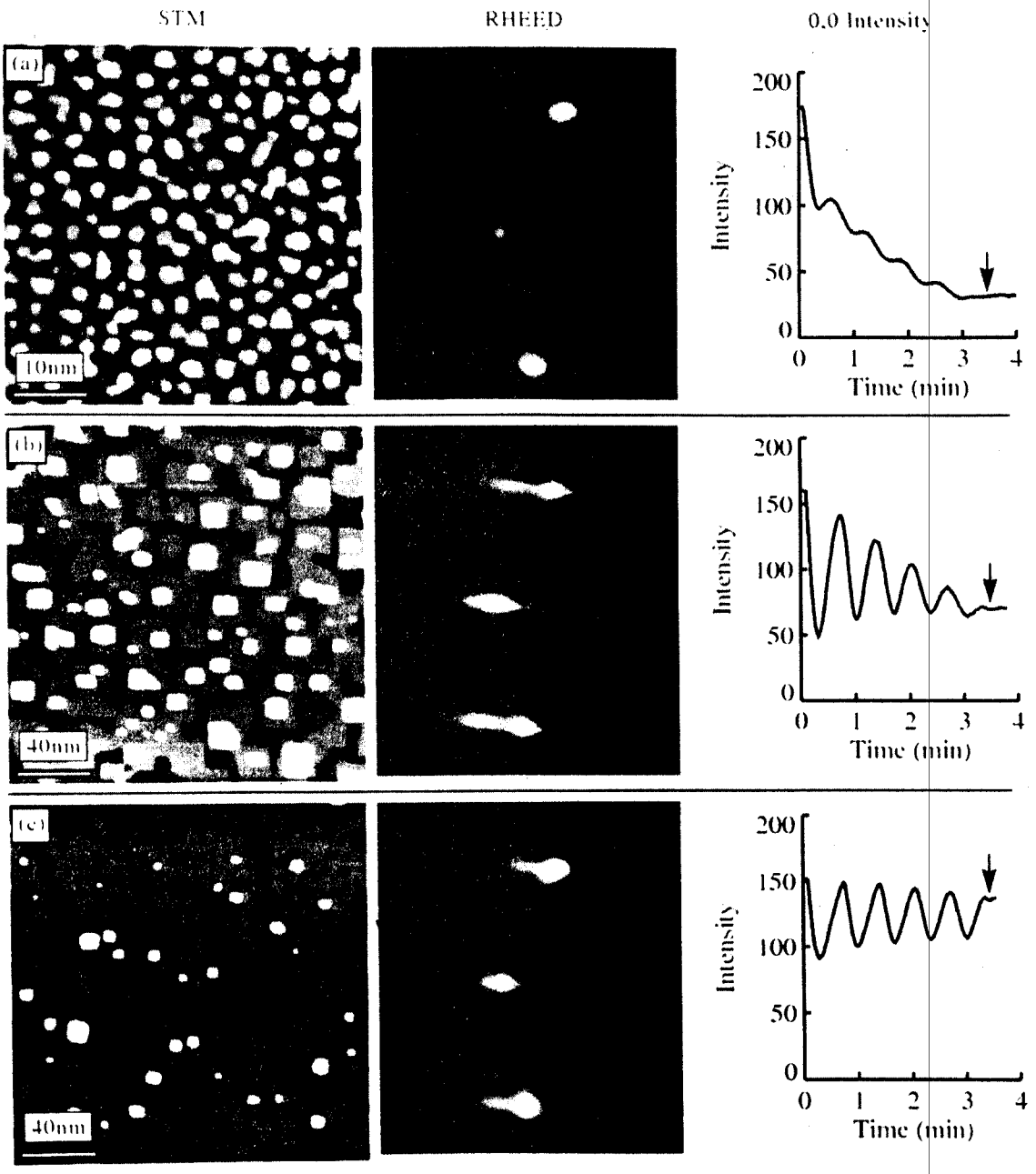

FIG. 7. STM image, RHEED diffraction patterns, and RHEED (0,0) beam intensity measurements of Fe on Fe(001) growth obtained on the same samples. All the films were grown for five RHEED oscillations, at which time the Fe flux was turned off, indicated by the arrows in the RHEED intensity plots. The RHEED measurements were made with a 10 keV beam at the antiphase angle of incidence of 64 mrad. The diffraction patterns consist of the (0,0), $(0,\bar{1})$, and $(\bar{1},0)$ spots, and are shown with a logarithmic intensity scale to highlight the low level intensities. The (0,0) intensity profiles were obtained by integrating over the (0,0) diffraction spot by $\pm 0.05°$ in both directions. Sample temperatures during growth, rms roughness, and step densities are (a) 20 °C, 0.116 nm, 1.74 nm^{-1}; (b) 180 °C, 0.095 nm, 0.24 nm^{-1}; (c) 250 °C, 0.06 nm, 0.09 nm^{-1}. STM images are shown in a grey scale with black being the lowest height level. The major changes in grey level indicate a monoatomic step. Image sizes are (a) 50×50 nm; (b), (c) 200×200 nm.

ACKNOWLEDGMENTS

We are grateful to R. J. Celotta, M. D. Stiles, and J. Unguris for helpful discussions, and R. A. Dragoset for his assistance. This work is supported by the Office of Technology Administration of the Department of Commerce and the Office of Naval Research. The Fe whiskers were grown at Simon Fraser University under an operating grant from the National Science and Engineering Research Council of Canada.

[1] J. A. Stroscio, D. T. Pierce, and R. A. Dragoset, Phys. Rev. Lett. **70**, 3615 (1993).
[2] J. A. Stroscio and D. T. Pierce, Phys. Rev. B **49**, 8522 (1994).
[3] M. C. Bartelt and J. W. Evans, Phys. Rev. B **46**, 12 675 (1992); J. W. Evans and M. C. Bartelt, Surf. Sci. **284**, L437 (1993); M. C. Bartelt, M. C. Tringides, and J. W. Evans, Phys. Rev. B **47**, 13 891 (1993); J. W. Evans and M. C. Bartelt, J. Vac. Sci. Technol. (to be published).
[4] Y.-W. Mo, J. Kleiner, M. B. Webb, and M. G. Lagally, Phys. Rev. Lett. **66**, 1998 (1991); Surf. Sci. **268**, 275 (1992).
[5] J. A. Stroscio, D. T. Pierce, R. A. Dragoset, and P. N. First, J. Vac. Sci. Technol. A **10**, 1981 (1992).

[6]A. S. Arrott, B. Heinrich, and S. T. Purcell, in *Kinetics of Ordering and Growth at Surfaces*, edited by M. G. Lagally (Plenum, New York, 1990), p. 321.
[7]R. Gomer, Rep. Prog. Phys. **53**, 917 (1990).
[8]See, for example, *Reflection High Energy Electron Diffraction and Reflection Electron Imaging of Surfaces*, edited by P. K. Larson and P. J. Dobson, NATO ASI Ser. B, Vol. 188 (Plenum, New York, 1988).
[9]J. H. Neave, B. A. Joyce, P. J. Dobson, and N. Norton, Appl. Phys. A **31**, 1 (1983); J. M. Van Hove, C. S. Lent, P. R. Pukite, and P. I. Cohen, J. Vac. Sci. Technol. B **1**, 741 (1983).
[10]S. Clarke and D. D. Vvedensky, Phys. Rev. Lett. **58**, 2235 (1987); J. Appl. Phys. **63**, 2272 (1988).
[11]J. Sudijono, M. D. Johnson, C. W. Snyder, M. B. Elowitz, and B. G. Orr, Phys. Rev. Lett. **69**, 2811 (1992).
[12]G. S. Petrich, P. R. Pukite, A. M. Wowchak, G. J. Whaley, P. I. Cohen, and A. S. Arrott, J. Cryst. Growth **95**, 23 (1989).
[13]P. I. Cohen, G. S. Petrich, P. R. Pukite, G. J. Whaley, and A. S. Arrott, Surf. Sci. **216**, 222 (1989).
[14]H. C. Kang and J. W. Evans, Surf. Sci. **271**, 321 (1992).